Planet. Space Sci., Vol. 32, No. 1, pp. 97–104, 1984
Printed in Great Britain.

0032-0633/84 $3.00 + 0.00
Pergamon Press Ltd.

EFFECTS OF THE DAYSIDE FIELD-ALIGNED CURRENTS IN LOCATION AND STRUCTURE OF POLAR CUSPS

N. A. TSYGANENKO and A. V. USMANOV
Institute of Physics, Leningrad State University, Leningrad 198904, U.S.S.R.

(*Received in final form* 26 *April* 1983)

Abstract—We have studied the dayside magnetosphere structure and its K_p-, A_E- and IMF-dependence using the magnetic data from IMP and HEOS satellites obtained during 1966–1972. An analysis of the field line configurations has been done on the basis of results of a least squares fitting of the model coefficients to the data subsets. The plots of the magnetopause subsolar point distance and of the polar cusp latitude vs K_p and A_E have been obtained. A detailed study of the model field distribution has revealed a substantial difference in the polar cusp field line geometry between the cases of weak and strong geomagnetic activity. We find that this results in a considerable longitudinal extension of the isointensity contours of particle precipitation at ionospheric heights during disturbed periods with $K_p \geqslant 3$ or $A_E \gtrsim 300$ nT. The same effect has been detected for the data subsets corresponding to the IMF $B_z < 0$. In contrast, at quiet times the precipitation isolines are much closer to circles. We conclude therefore that the cleft-like structure of polar cusps pertains only to active periods and can be explained by a magnetic effect of enhanced Birkeland currents.

INTRODUCTION

Recent investigations (Reiff *et al.*, 1977; Haerendel *et al.*, 1978; see also reviews by Roederer, 1979; Sergeev and Tsyganenko, 1980) have established the importance of physical phenomena in the polar cusp and entry layer regions responsible for the solar wind particle and field penetration into the magnetosphere. The main results concerning the location and structure of polar cusps, as well as their response to changes in the solar wind state, have been obtained from measurements of charged particles, due to a number of clearly identifiable signatures in the flux spatial distribution and energy spectra. Using the magnetic data for studies of the polar cusps is a more sophisticated task because of difficulties in interpretation of a spacecraft's measurements, which correspond to a net magnetic effect taking contribution from several sources distributed over a wide volume. For this reason only statistical quantitative modeling methods based on a sufficiently extended data set can provide a reliable result.

Of particular interest is the question on the longitudinal extension of the polar cusp region, which remains as yet a subject of controversy. Heikkila and Winningham (1971) have proposed the concept of the magnetospheric cleft; this type of structure implies the existence of a sufficiently long demarcation line at the magnetopause, being the border between the dayside closed force lines and those swept down into the tail region. An opposite point of view has been developed recently by Sauvaud *et al.* (1980) on the basis of their results of particle measurements on board the *Aureole-1* satellite. According to their data, the polar cusp projection on the ionosphere looks like a spot, rather than a long band and hence, the cleft concept should be revised. Zaitzeva and Pudovkin (1976) have presented evidence for an increase of the polar cusp longitudinal extension during disturbed periods.

In the present paper the large-scale structure of the polar cusp region is studied using the results of modeling the dayside magnetosphere based on data from four IMP and two HEOS satellites obtained during 1966–1972. The initial data set including about 19,000 vector averages was the same as that used by Tsyganenko and Usmanov (1982) for derivation of parameters of a series of 'global' (in the sense of comprising both the dayside and the nightside regions) magnetospheric field models. Due to selection of measurements made within the sector $|\lambda_{SM}| \leqslant 60°$, we have substantially reduced the initial data set, so that the set used in this 'local' model study included in total only about 4000 data points distributed within the dayside region.

LATITUDINAL POSITION OF POLAR CUSPS VS GROUND ACTIVITY LEVEL

We have been particularly interested in obtaining a more accurate model representation of the magnetic field in a relatively limited magnetospheric region; it was decided therefore to introduce the cubic polynominals in solar magnetic Cartesian coordinates

for fitting the extraterrestrial current contribution to the measured magnetic field:

$$
\begin{aligned}
B_x &= (a_1 + a_2 x + a_3 z^2 + a_4 x^2 + a_5 y^2) z \\
&\quad + [a_6 + a_7 x + a_8 x^2 + a_9 y^2 + a_{10} z^2 \\
&\quad + (a_{11} x^2 + a_{12} y^2 + a_{13} z^2) x] \sin \psi \\
B_y &= y[(b_1 + b_2 x) z + \sin \psi (b_3 + b_4 x \\
&\quad + b_5 y^2 + b_6 x^2 + b_7 z^2)] \\
B_z &= c_1 + c_2 x + c_3 x^2 + c_4 y^2 + (c_5 y^2 + c_6 x^2) x \\
&\quad + (c_7 + c_8 x) z^2 + z \sin \psi (c_9 + c_{10} x \\
&\quad + c_{11} z^2 + c_{12} x^2 + c_{13} y^2).
\end{aligned} \tag{1}
$$

The model expansions (1) comprise the contribution from all extraterrestrial sources, including the magnetopause currents, the tail current sheet, the field-aligned currents and the ring current. The last two sources have the smallest variation scale of B in the model region and hence, a substantial smoothing away of their fine structure details should be expected due to a relative simplicity of the model formulae (1). Nevertheless, as it will be shown below, the obtained gross pattern of the model current distribution still can provide a clear indication of the field-aligned currents as the main intramagnetospheric source contributing to the observed structure of the dayside magnetospheric field.

The model coefficients a_1–a_{13}, b_1–b_7, and c_1–c_{13} have been derived by means of a standard least squares technique, with imposition of the div $\mathbf{B} = 0$ requirement. Note that proper dawn–dusk and North–South symmetry conditions are taken into account in (1), being similar to those applied by Mead and Fairfield (1975) (see their equations 1–6). We have determined the values of the model coefficients for a series of data subsets corresponding to different levels of the geomagnetic activity and for two polarities of the B_z-component of the interplanetary magnetic field. After that the position of the neutral points of the magnetic field and their ionospheric projections have been found using a field line tracing procedure. Figure 1a shows the latitude of ionospheric projection of the model polar cusps, ϕ_c and the subsolar point distances, R_s, plotted vs K_p-index. Each point of the curves corresponds to a data subset comprising from ~ 500 up to ~ 1400 vector averages of the measured field. It should be noted also that, for every point in Fig. 1a, the data corresponding to the nearest neighbour values of the K_p have been included also in the data subset; thus, for example, the point with $K_p = 1^+$ has been obtained from the subset containing the measurements taken by $K_p = 1, 1^+$ and 2^-. Therefore, the points in Fig. 1a are not completely independent of each other. It appeared necessary to use such overlapping subsets because of lack of measurements; a relative scarcity of data points for the separate K_p values leads to their spatial inhomogeneity and hence, to an undesirable scatter in the calculated model coefficients. Figure 1b shows the same quantities, as in Fig. 1a, derived for different intervals of the A_E-index. The size of horizontal bars marks the A_E-index range corresponding to each data subset.

Besides sorting the data in accordance with the ground activity indices, we have carried out a study of effects in the model dayside magnetosphere due to changes in the IMF polarity. Two subsets have been compiled from the original data set, corresponding to the positive and negative polarities of the hourly averaged B_z-component during a given and preceding hour. The last requirement has been imposed with the aim to remove a possible contribution from intermediate cases, i.e. transient periods of short duration and to reveal more clearly the temporally accumulating effects. We have obtained for $B_z \geqslant 0$ and $B_z < 0$, respectively, $\phi_c^+ = 79.75°$, $R_s^+ = 12.24\ Re$ and $\phi_c^- = 77.65°$, $R_s^- = 11.51\ Re$. The first data subset has the average $\bar{K}_p$ between 1^+ and 2^- and $A_E = 85.5$ nT, whereas the second one, as it should be expected, corresponds to a more disturbed state having $\bar{K}_p \approx 2^+$ and $A_E = 255$ nT.

As can be seen from these results, the following well-known facts are clearly manifested in the structure of our model geomagnetic field: the increase in the ground disturbancy level, as well as the southward change in the IMF B_z polarity, lead to an equatorward shift of polar cusps and to a decrease of the subsolar point distance. Similar features have been observed also in the model investigations by Mead and Fairfield (1975) and by Tsyganenko and Usmanov (1982). In the present study, however, we have restricted the modeling region by taking the data from the dayside sector only, which provided a more accurate representation of the daytime magnetic field due to exclusion of the influence of the nightside data points on the model coefficients.

The model coefficients obtained for various K_p and A_E intervals are given in Tables 1 and 2.

LONGITUDINAL STRUCTURE OF POLAR CUSPS

We note first of all that the configuration of the magnetospheric boundary layer magnetic field lines in the region of their convergence into the polar cusp bundle and in particular, the longitudinal extension of the cusp 'throat' is related to the shape of isolines of the total magnetic field magnitude, B, just below the magnetopause. To clarify this point, let us consider the

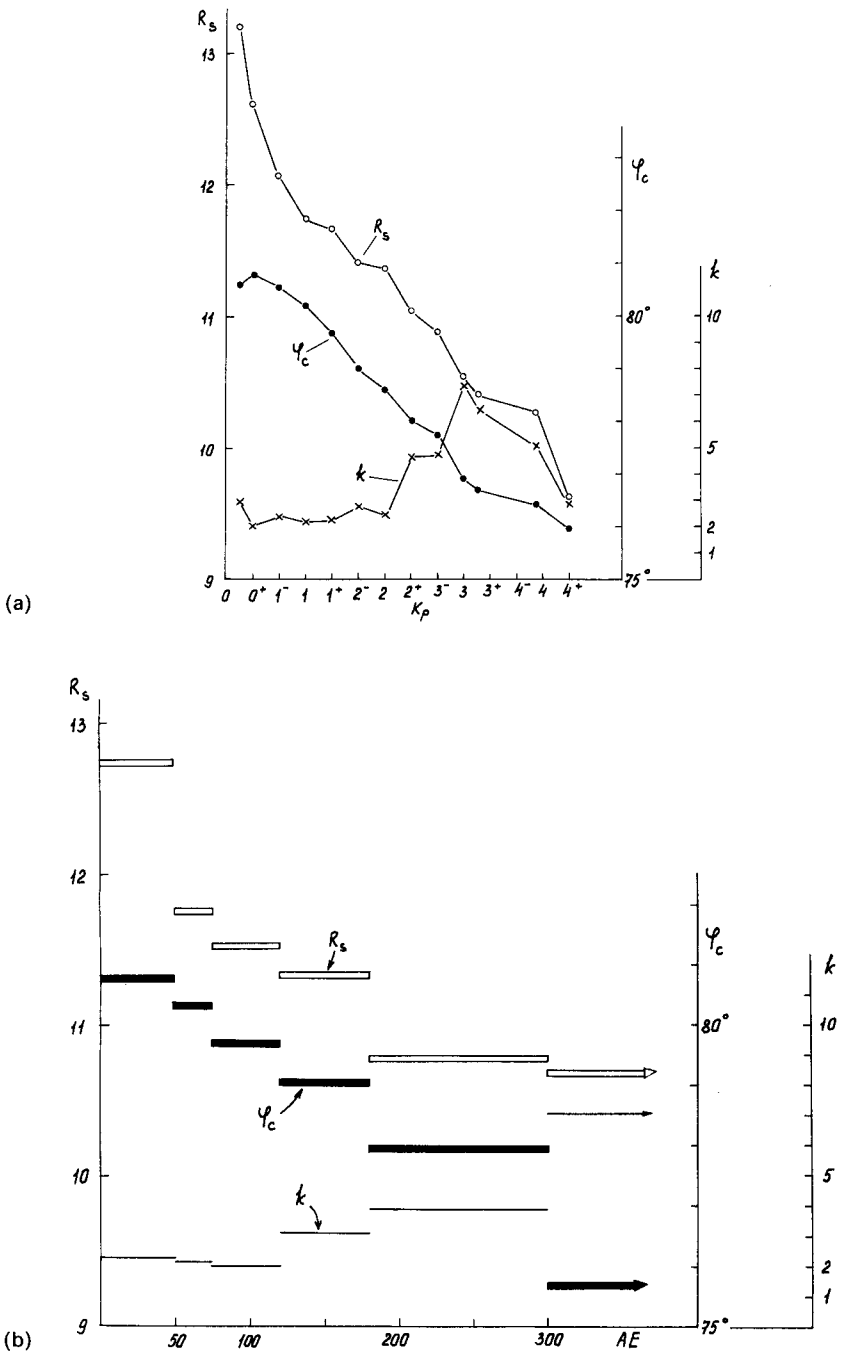

FIG. 1. PLOTS OF THE SUBSOLAR POINT DISTANCE, R_s (OPEN CIRCLES AND OPEN BARS), POLAR CUSP IONOSPHERIC LATITUDE, ϕ_c (SOLID CIRCLES AND SOLID BARS), AND THE ELONGATION COEFFICIENT, k, OF THE B-ISOLINES MAPPED FROM THE MODEL MAGNETOPAUSE ONTO THE IONOSPHERE (CROSSES AND THIN BARS), VS THE K_p-INDEX (a) AND A_E-INDEX (b).

TABLE 1. COEFFICIENTS OF EXPANSION (1) FOR A SERIES OF K_p INTERVALS. THE NUMBER OF DATA POINTS IN THE DATA SUBSET, N AND THE R.M.S. DEVIATION OF THE MODEL FIELD FROM THE DATA, σ, ARE GIVEN AT THE TOP OF EACH COLUMN

K_p	$0, 0^+, 1^-$	$0^+, 1^-, 1$	$1^-, 1, 1^+$	$1, 1^+, 2^-$	$1^+, 2^-, 2$	$2^-, 2, 2^+$	$2, 2^+, 3^-$	$2^+, 3^-, 3$	$3^-, 3, 3^+$	$\geqslant 3$	$> 3^+$
N	788	1139	1370	1410	1396	1222	1028	844	679	770	349
σ	11.87	12.84	13.64	13.45	13.78	13.42	13.91	16.57	20.34	22.84	21.04
a_1	2.865	3.156	3.466	3.819	3.942	4.094	3.991	4.497	4.941	5.576	6.676
a_2	−0.1943	−0.09281	−0.1673	−0.2585	−0.2581	−0.1148	0.01288	0.02889	0.04788	0.3423	0.5194
a_3	0.00168	−0.00254	−0.00396	−0.00381	−0.00274	−0.00282	−0.00373	−0.00699	−0.01088	−0.0162	−0.0252
a_4	0.00005	−0.01264	−0.00376	0.00370	0.00541	−0.0127	−0.0204	−0.02209	−0.02319	−0.06347	−0.08775
a_5	−0.01288	−0.01945	−0.02707	−0.02979	−0.03385	−0.0333	−0.03881	−0.04193	−0.05339	−0.05231	−0.07524
a_6	−3.356	12.54	19.06	29.73	22.60	21.88	29.14	36.43	38.19	54.76	88.76
a_7	9.599	4.709	3.912	0.3967	2.639	0.3458	−0.8817	0.4699	1.854	−6.727	−19.00
a_8	−1.985	−1.268	−1.290	−0.8407	−0.9990	−0.3231	−0.09491	−0.8211	−1.509	−0.2050	1.696
a_9	−0.2384	−0.5306	−0.7121	−0.8688	−0.9891	−0.6972	−0.9093	−0.7550	−0.8418	−0.1766	−0.7012
a_{10}	0.2548	0.06032	0.00972	0.01971	0.1052	0.09809	−0.0248	−0.06357	−0.1852	−0.3410	−0.7634
a_{11}	0.1030	0.06005	0.06491	0.04409	0.04525	0.00399	−0.01463	0.03886	0.08455	0.01733	−0.1000
a_{12}	0.0209	0.05530	0.07520	0.08942	0.09971	0.0498	0.06731	0.04484	0.06902	−0.0140	0.08682
a_{13}	−0.03414	−0.01358	−0.02024	−0.01642	−0.01827	−0.01372	0.02091	0.03216	0.07814	0.1391	0.2806
b_1	−0.2571	−0.2083	−0.2339	−0.2373	−0.2364	−0.2304	−0.2100	−0.2093	−0.2683	−0.3409	−0.2960
b_2	0.02756	0.01715	0.02123	0.02083	0.02317	0.02314	0.02623	0.02988	0.04913	0.04233	−0.00387
b_3	−13.02	−7.482	−6.075	−2.995	−6.055	−4.721	−5.484	−5.378	−10.51	−3.324	−0.6512
b_4	3.082	1.702	1.369	0.7594	1.573	1.095	1.214	1.152	3.256	0.6243	−0.6908
b_5	−0.00326	−0.00521	−0.00663	−0.01364	−0.01474	−0.01011	−0.00565	0.00484	−0.01489	0.00209	0.02286
b_6	−0.1900	−0.1052	−0.08285	−0.04989	−0.1028	−0.06841	−0.07136	−0.07033	−0.2267	−0.03486	0.05063
b_7	0.00649	−0.00486	−0.01374	−0.02192	−0.01096	−0.00357	0.00192	−0.00105	−0.00973	−0.03814	−0.05594
c_1	−19.43	−14.78	−19.74	−21.74	−22.30	−19.76	−16.09	−20.14	−21.04	−5.072	−2.520
c_2	6.965	3.843	4.599	2.730	2.407	2.159	0.5364	2.695	0.08092	−14.80	−19.74
c_3	−0.4727	0.04671	0.03896	0.4914	0.6009	0.5165	0.7878	0.6267	1.183	4.253	5.329
c_4	−0.05493	0.06613	0.1687	0.3188	0.3086	0.2798	0.2758	0.2892	0.6072	0.6208	0.3142
c_5	0.01692	−0.00391	−0.01926	−0.03428	−0.03587	−0.02908	−0.03783	−0.04530	−0.08112	−0.07712	−0.04551
c_6	0.01305	−0.00937	−0.00901	−0.03294	−0.03886	−0.03168	−0.04418	−0.0479	−0.07101	−0.2515	−0.3115
c_7	0.2257	0.1506	0.2006	0.2479	0.2472	0.1726	0.09856	0.09021	0.1102	−0.00071	−0.1117
c_8	−0.01383	0.00407	−0.00685	−0.01411	−0.017	0.00113	0.00729	0.00715	−0.00138	0.0423	0.08968
c_9	3.418	2.772	2.163	2.598	3.416	4.375	6.366	4.908	8.657	10.05	19.65
c_{10}	0.8877	0.8329	1.2102	0.922	0.4246	−0.4488	−1.024	0.4900	−0.2394	−0.2144	−2.702
c_{11}	0.00922	0.00615	0.01133	0.01278	0.00975	0.00577	−0.00761	−0.01037	−0.0288	−0.03366	−0.07489
c_{12}	−0.119	−0.07494	−0.1119	−0.08239	−0.03289	0.05645	0.1152	−0.04626	−0.02692	−0.01713	0.2494
c_{13}	−0.0111	−0.03966	−0.0553	−0.04849	−0.0555	−0.01947	−0.05037	−0.05937	−0.02435	0.00774	−0.1554

TABLE 2. THE SAME, AS IN TABLE 1, FOR SEVERAL INTERVALS OF A_E-INDEX AND FOR TWO POLARITIES OF THE INTERPLANETARY MAGNETIC FIELD Z-COMPONENT

A_E	50 nT	50–75	75–120	120–180	180–300	300	$B_z \geq 0$	$B_z < 0$
N	612	669	732	657	620	706	539	537
σ	10.52	13.36	13.02	14.01	16.24	20.63	14.81	17.19
a_1	2.900	3.026	3.639	4.855	4.576	5.815	3.485	4.339
a_2	−0.2335	−0.2782	−0.2530	−0.2243	0.1376	0.2511	−0.05291	0.1579
a_3	0.00101	0.00292	−0.00361	−0.0071	−0.00906	−0.02122	−0.00260	−0.0095
a_4	0.00276	0.00993	0.00809	−0.01011	−0.03682	−0.05246	−0.01424	−0.04428
a_5	−0.00849	−0.0177	−0.03624	−0.03865	−0.0459	−0.03979	−0.03725	−0.03476
a_6	−3.743	16.32	26.32	39.43	40.83	52.61	7.910	53.02
a_7	3.554	3.386	0.3604	−1.7323	2.631	−5.346	7.988	2.573
a_8	−0.6787	−1.3204	−0.8490	−0.5843	−1.638	0.1917	−2.1869	−1.742
a_9	−0.1298	−0.4995	−0.6839	−0.9005	−1.1428	−0.2926	−0.5929	−1.461
a_{10}	0.2459	0.03439	−0.07975	−0.00284	−0.1582	−0.6734	0.1011	−0.2618
a_{11}	0.03407	0.07086	0.04934	0.02773	0.08470	−0.02573	0.1261	0.09179
a_{12}	0.00891	0.05943	0.05439	0.08942	0.1266	−0.01348	0.0360	0.1552
a_{13}	−0.03788	−0.00849	0.00899	−0.00594	0.04825	0.1690	−0.00157	0.02998
b_1	−0.2239	−0.2884	−0.2216	−0.2164	−0.3143	−0.3697	−0.4238	−0.1770
b_2	0.02306	0.03099	0.01917	0.01765	0.04137	0.06056	0.05757	0.01692
b_3	−7.2928	−7.986	−3.360	−2.063	−8.509	−11.71	−11.89	−3.797
b_4	1.2657	2.004	0.7297	0.5004	2.368	2.967	3.031	1.173
b_5	−0.00277	−0.01056	−0.00343	−0.02261	−0.01009	0.01553	−0.00975	−0.02313
b_6	−0.05413	−0.1230	−0.05117	−0.02971	−0.1707	−0.1979	−0.1733	−0.07709
b_7	0.00496	−0.00395	−0.02843	−0.03171	−0.01980	0.01144	−0.01787	−0.02073
c_1	−17.22	−27.77	−22.99	−18.89	−21.35	−27.88	−26.03	−10.42
c_2	3.818	8.045	4.9305	−0.3337	2.392	−4.151	8.009	−6.287
c_3	0.1240	−0.3395	0.0827	1.3031	0.8112	2.210	−0.2397	1.945
c_4	0.1019	0.2559	0.2906	0.3903	0.2890	0.4672	0.2454	0.5047
c_5	−0.00526	−0.0332	−0.02308	−0.05283	−0.04161	−0.0529	−0.02847	−0.05025
c_6	−0.01653	0.00498	−0.01290	−0.08674	−0.06094	−0.1323	−0.01399	−0.1034
c_7	0.2287	0.2833	0.2373	0.2204	0.08834	0.05934	0.2383	0.00954
c_8	−0.01429	−0.02542	−0.01767	0.00128	0.01613	0.02218	−0.01454	0.03582
c_9	3.7388	4.6005	2.000	3.796	5.878	17.06	3.901	1.224
c_{10}	0.09158	0.6366	0.9684	0.6683	0.9078	−3.351	1.342	2.310
c_{11}	0.01098	0.00415	0.00648	0.01255	−0.00948	−0.06015	0.00648	−0.00308
c_{12}	−0.04809	−0.08960	−0.09687	−0.05347	−0.08345	0.2751	−0.2050	−0.1983
c_{13}	−0.00061	−0.02775	−0.04410	−0.02158	−0.09629	−0.03311	−0.00676	−0.08583

following examples. In a spherical model magnetosphere we have two neutral points, which lie in the focuses of a family of circular B-isolines centered at the axis of symmetry. In the Chapman–Ferraro model with a planar magnetopause these isolines are close to ellipses (in a sufficiently small vicinity of the cusp region) with the ratio of major to minor axes being about 4 : 3. A cylindrical model (an axially symmetric configuration with a dipole inside a cylindrical cavity of infinite length) represents an opposite limiting case, in which the B-isolines are torn and reconnected in such a way that they form a family of circles girding the cavity, the neutral points being transformed into a pair of circular neutral lines, corresponding to the $B = 0$ isolines.

Based on the last example, we can state that the longitudinal extension of polar cusps depends, in particular, on the degree of axial symmetry of the magnetic field from extraterrestrial sources about the geodipole axis near the 'throat' region (the spherical model is a degenerate case in this sense, because its neutral points lie at the symmetry axis). As the external magnetic field in the dayside sector changes towards a more axially symmetric configuration, the B-isolines around the neutral points must exhibit an additional elongation in the azimuthal direction. Obviously, such a reconfiguration of the outer magnetic force lines should be manifested in a certain changes of the distribution of cusp-related geophysical phenomena at ionospheric heights.

To obtain a quantitative solution of the problem of solar wind particle penetration into the cusps, it is necessary to specify the injection mechanisms, as well as to know the electric field distribution and some other factors. We have used in this study a simple method based on an assumption that the efficiency and a characteristic depth of the particle penetration across

the near-cusp magnetopause are controlled mainly by the module of the total magnetic field at the injection point. According to this statement, the following procedure for determination of the gross pattern of particle precipitation intensity at ionospheric level has been developed. Having determined the position of the model magnetospheric boundary, we find one of B-isolines at the magnetopause and shift all its points inside the magnetosphere along the normal to the surface by the distance ΔL, of the order of a characteristic particle penetration depth. The shifted isoline is then mapped down along the model field lines up to the ionospheric level; the obtained contour can be interpreted as an isoline of the precipitation flux intensity. As it will be shown below, such an approach, despite its limitations and simplicity, can shed light upon the role of geometrical properties of the high-latitude geomagnetic field in formation of the dayside auroral zone and reveals some remarkable features corresponding to transition from quiet to disturbed conditions.

We have chosen in our calculations a $B = 5$ nT isoline at the model magnetopause, the characteristic injection depth being assumed equal to $\Delta L = 0.3\ Re$; considering the last value to be a proton gyroradius, we obtain an estimate for the particle energy $w \sim 2$ keV. The model magnetopause was found in each case using a 2-fold procedure. At the first stage a numerical computation of a field line bundle passing through a small vicinity of the neutral point was carried out; we obtained thus a family of magnetic force lines lying at the magnetopause and providing more or less uniform distribution of boundary points around the cusp region within radial distance from the latter of about 4 Re. At the second stage the coefficients of a polynomial in y and z were found as a result of the least squares fitting of a fourth-order algebraic surface to the magnetopause points obtained at the first stage, the r.m.s. deviation of this surface from the bundle field line points being not more than 0.0008 Re in all cases. Having found the analytical approximation for the model magnetopause, we applied a numerical procedure, which determined an isoline of B at the surface, then shifted the obtained contour into the magnetosphere by a given distance, ΔL, and finally, traced it down onto the ionosphere using a standard Runge–Kutta technique.

Figure 2 shows the results of mapping of $B = 5$ nT isoline onto the ionosphere by means of the outlined above procedure. The upper and the lower contours correspond, respectively, to quiet ($K_p = 1^-, 1, 1^+$) and moderately disturbed ($K_p = 3^-, 3, 3^+$) versions of the model magnetic field (1). In the last case we see a marked elongation of the contour, as compared to that pertaining to quiet conditions, the ratio of longitudinal to latitudinal dimension of the contour being $k = \Delta y/\Delta x \approx 7$ for $K_p = 3^-, 3, 3^+$, whereas $k \approx 2$ for $K_p = 1^-, 1, 1^+$. It should be noted also that the elongation of the corresponding B-isolines at the magnetopause is considerably smaller, the ratios of their major to minor axes being ≈ 2.3 in disturbed and ≈ 1.2 in quiet model versions. Therefore, the observed stretching of the ionospheric contours in longitudinal direction should be explained by specific properties of the geomagnetic field line geometry in the outer dayside magnetosphere, rather than by existence of a 'demarcation line' at the magnetopause. We emphasize also that the main contribution to this effect should apparently be ascribed to the field-aligned currents flowing in the vicinity of polar cusps, since we failed to obtain a similar feature in calculations with models containing no such sources; thus, the image-dipole model gave no more than $k \approx 1.8$. The observed peculiarity can be somewhat clarified by an inspection of values of the model coefficients b_1 and b_2 from (1). The model version for $K_p = 1^-, 1, 1^+$, which yielded the minimum elongation (the upper contour in Fig. 2) has $b_1 = -0.234$ and $b_2 = 0.021$, so that in the outer cusp region ($x \sim 7$–10 Re) we have, by $\psi = 0: B_y \approx -0.06yz$. In the second case ($K_p = 3^-, 3, 3^+$; the lower contour in Fig. 2) $b_1 = -0.268$ and $b_2 = 0.049$, so that $B_y \approx +0.15yz$ in the same region. Taking into account the negative sign of B_x in both cases, we conclude that in the first case the force lines of the external field (1) diverge from the midday meridional plane in the antisolar direction, whereas in the second case they converge. As a consequence, the total magnetic field in the last case shows a higher degree of axial symmetry about the z-axis, than that in the first case, which explains, in line with the above developed arguments, the observed lengthening of the polar cusp projection.

Contours, similar to those shown in Fig. 2, have been computed for all intervals of activity indices and for two IMF polarities. The results are plotted in Fig. 1, showing the dependence of the quantity k on the disturbancy level, that is, vs K_p (crosses in Fig. 1a) and A_E (thin solid bars in Fig. 1b). The most notable feature in both cases is a clear tendency for k to rise with the increase of activity from very quiet to moderately disturbed conditions. However, as can be seen from Fig. 1a, a further increase of the K_p-index from 3 to 4^+ is accompanied by a monotonous decrease of the elongation coefficient, k, whereas no such behaviour had been found in the corresponding A_E plot. We tried to explain this difference by an assumption that the large K_p values refer mainly to later stages of disturbances, when the ring current is the most intense, whereas the high-latitude field-aligned currents (associated predominantly with the development and

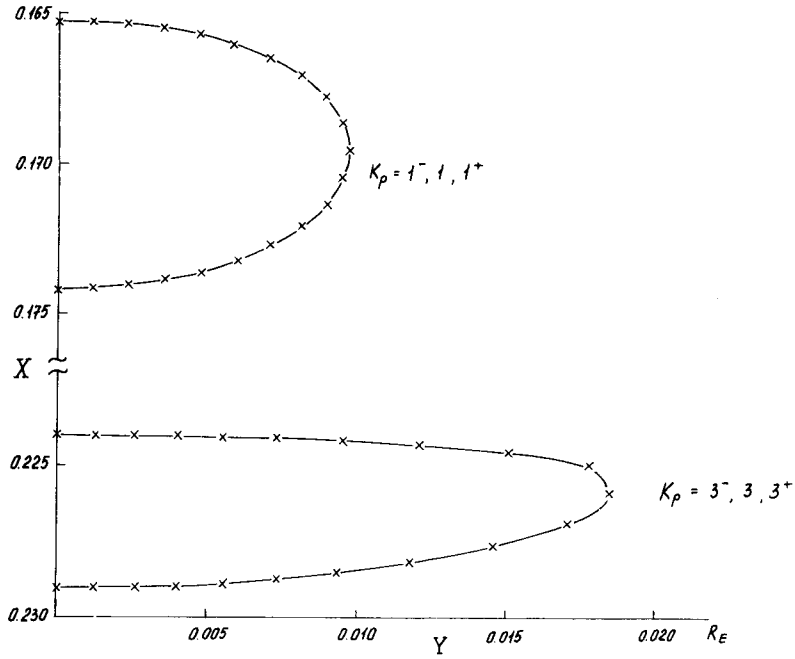

FIG. 2. THE CONTOURS AT THE IONOSPHERIC LEVEL, OBTAINED FROM THE $B = 5$ nT ISOLINE AT THE MAGNETOPAUSE BY MEANS OF THE TRACING PROCEDURE, DESCRIBED IN THE TEXT, FOR QUIET (ABOVE) AND MODERATELY DISTURBED (BELOW) DAYSIDE MODEL MAGNETOSPHERE.
Due to symmetry with respect to X-axis, only the right halves of contours are shown.

explosive phases of a substorm) are already rather weak. An additional run for a data subset with $A_E > 330$ nT has shown, however, that the elongation also lessens down to $k \approx 3.3$ in this case. We suspected then the data subsets for the high activity levels to be of an insufficient informative capability, due to a scarcity of the data points; thus, the subset for $K_p > 3^+$ includes only 349 points, in comparison with 600–1400 points typical for lower K_p intervals. It seems, however, that the main and the most likely reason for the decrease in k at higher K_p and A_E is a much greater variability of the dayside magnetopause and polar cusp position during active periods, which should result in an averaging out of the details of the field distribution.

Data subsets, corresponding to different IMF polarities gave the following values of k: $k \approx 2.2$ for $B_z \geqslant 0$, and $k \approx 4.9$ for $B_z < 0$ (the IMF polarity, again, was required to be the same during a given and preceding hour).

We now consider briefly the structure of distributed currents responsible for the observed changes of the dayside geomagnetic field. Taking the curl of the model field (1) and substituting the numerical values of coefficients for the case $A_E > 300$ nT from Table 2, we yield the components of the current density (in arbitrary units):

$$j_x = 1.304y - 0.1664xy,$$

$$j_y = 9.966 - 4.17x + 0.344x^2 + 0.0131y^2 - 0.858z^2,$$

$$j_z = 0.14yz.$$

We have computed a family of the current flow lines corresponding to these expressions; the result is shown in Fig. 3. As can be seen from Fig. 3a (the current flow pattern in the equatorial plane), the lines of **j** have a vortical structure, the major vortex being centered at $x \sim 3.5\,Re$. Figure 3b shows a number of current loops in projection onto the midday meridian plane, the magnetopause position being indicated by a dashed line with the asterisk showing the location of the magnetic neutral point. Now it is clearly seen that the current flow lines descend from the outer polar cusp region in the prenoon sector, cross the midday meridian plane at lower altitudes, and then ascend again towards the magnetopause. We interpret this picture as a clear indication of the high-latitude field-aligned current circuit, though significantly averaged in space and time

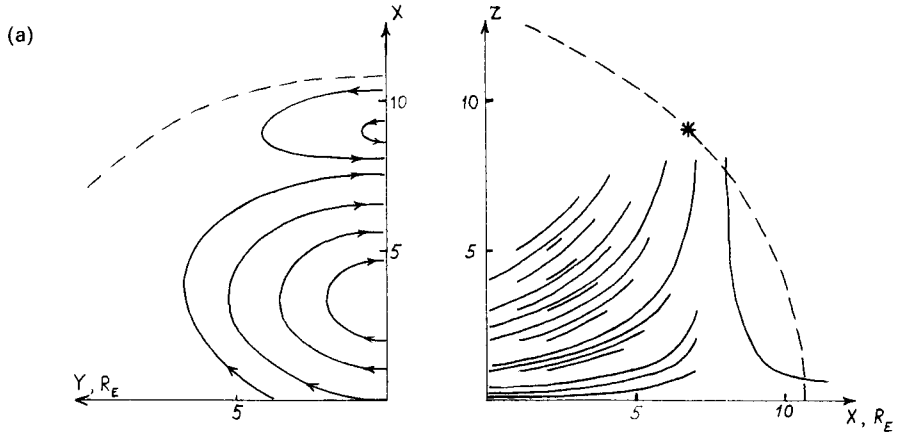

FIG. 3. THE MODEL CURRENT FLOW LINES FOR THE $A_E > 300$ nT VERSION: (a) THE CURRENT LINE PATTERN IN THE EQUATORIAL PLANE; (b) THE CURRENT FLOW LINES AS VIEWED IN PROJECTION ONTO THE MIDDAY MERIDIAN PLANE. The magnetopause position is shown by dashed line; the asterisk in Fig. 3b indicates the location of the magnetic neutral point.

due to inevitable model limitations. The net magnetic effect of these currents is to decrease the total field in the dayside low-latitude magnetosphere and to increase the magnetic flux swept into the tail through the high-latitude regions.

At last, some words should be said on the influence of the B_y-component of the IMF on the model magnetospheric field. We investigated this question by introducing more general cubic expansions for B_x, B_y and B_z containing the terms asymmetric with respect to the midday meridian plane. Having compiled two data subsets with $B_y^{IMF} \geqslant 0$ and $B_y^{IMF} < 0$, we computed the model coefficients and then determined the position of the dayside netural points; tracing them onto the ionosphere along the model magnetic force lines has yielded the longitudinal shift of the polar cusp footpoint for both polarities of the B_y^{IMF}, with the following result: $\lambda_c = 7.38°$ for $B_y^{IMF} \geqslant 0$ and $\lambda_c = -4.32°$ for $B_y^{IMF} < 0$ (the latitudes, ϕ_c, being equal to 78.54 and 78.74°, respectively). The obtained signs of λ_c are in agreement with those inferred from simple considerations of the reconnection geometry (e.g. Cowley, 1973).

In summary, we conclude that the location and structure of the polar cusp region and of the related dayside auroral precipitation zone is governed mainly by the field-aligned currents, the longitudinal extension of the daytime precipitation zone being determined by specific features of the field line geometry in the outer high-latitude magnetosphere, rather than by existence of a 'demarcation line' or a cleft-like slit at the magnetopause.

Acknowledgement—We are indebted to Dr. P. C. Hedgecock for providing us with the HEOS magnetic data. The IMP data used in this analysis were obtained through the services of the NSSDC and the World Data Center A for Rockets and Satellites. We also thank Prof. M. I. Pudovkin for stimulating discussions.

REFERENCES

Cowley, S. W. H. (1973) A qualitative study of the reconnection between the Earth's magnetic field and an interplanetary field of arbitrary orientation. *Radio Sci.* **8**, 903.

Crooker, N. U. (1977) The magnetospheric boundary layer: A geometrically explicit model. *J. geophys. Res.* **82**, 3629.

Haerendel, G., Paschmann, G. and Sckopke, N. (1978) The frontside boundary layer of the magnetosphere and the problem of reconnection. *J. geophys. Res.* **83**, 3195.

Heikkila, W. J. and Winningham, J. D. (1971) Penetration of magnetosheath plasma to low altitudes through the dayside magnetospheric cusps. *J. geophys. Res.* **76**, 883.

Mead, G. D. and Fairfield, D. H. (1975) A quantitative magnetospheric model derived from spacecraft magnetometer data. *J. geophys. Res.* **80**, 523.

Reiff, P. H., Hill, T. W. and Burch, J. L. (1977) Solar wind plasma injection at the dayside magnetospheric cusp. *J. geophys. Res.* **82**, 479.

Roederer, J. G. (1979) Global problems of magnetospheric plasma and prospects for their solution, in *Solar System Plasma Physics* (Edited by Kennel, C. F. *et al.*). North-Holland, Amsterdam.

Sauvaud, J.-A., Galperin, Yu. I., Gladyshev, V. A., Kuzmin, A. K., Muliarchik, T. M. and Crasnier, J. (1980) Spatial inhomogeneity of magnetosheath proton precipitation along the dayside cusp from the ARCADE experiment. *J. geophys. Res.* **85**, 5105.

Sergeev, V. A. and Tsyganenko, N. A. (1980) *The Earth's Magnetosphere*. Nauka, Moscow.

Tsyganenko, N. A. and Usmanov, A. V. (1982) Determination of the magnetospheric current system parameters and development of experimental geomagnetic field models based on data from IMP and HEOS satellites. *Planet. Space Sci.* **30**, 985.

Zaitzeva, S. A. and Pudovkin, M. I. (1976) On the longitudinal extent of the polar cusp. *Planet. Space Sci.* **24**, 518.